Published in final edited form as:
Stem Cells. 2009 August ; 27(8): 2032–2043. doi:10.1002/stem.119.

EGF induces the progeny of subventricular zone type B cells to migrate and differentiate into oligodendrocytes

Oscar Gonzalez-Perez[1,2,3], **Ricardo Romero-Rodriguez**[1], **Mario Soriano-Navarro**[4], **Jose Manuel Garcia-Verdugo**[4], and **Arturo Alvarez-Buylla**[1]

[1]Department of Neurological Surgery. Brain Tumor Research Center. Institute for Regeneration Medicine. University of California, San Francisco, 94143. U.S.A

[2]Laboratory of Neuroscience. School of Psychology. University of Colima. Colima, Col. 28040, Mexico

[3]Neuroscience Department, CUCS. University of Guadalajara. Guadalajara, Jal 44340, Mexico

[4]Laboratorio de Morfología Celular. Unidad Mixta CIPF-UVEG. 46013 Valencia, CIBERNED, Spain

Abstract

New neurons and oligodendrocytes are continuously produced in the subventricular zone (**SVZ**) of adult mammalian brains. Under normal conditions, the SVZ primary precursors (type B1 cells) generate type C cells, the majority of which differentiate into neurons, with a small sub-population giving rise to oligodendrocytes. Epidermal growth factor (**EGF**) signaling induces dramatic proliferation and migration of SVZ progenitors, a process that could have therapeutic applications. However, the fate of cells derived from adult neural stem cells after EGF stimulation remains unknown. Here, we specifically labeled SVZ B1 cells and followed their progeny after a 7-day intraventricular infusion of EGF. Cells derived from SVZ B1 cells invaded the parenchyma around the SVZ into striatum, septum, corpus callosum, and fimbria-fornix. The majority of these B1-derived cells gave rise to cells in the oligodendrocyte lineage including local NG2+ progenitors, pre-myelinating and myelinating oligodendrocytes. SVZ B1 cells also gave rise to a population of highly branched S100β+/GFAP+ cells in the striatum and septum, but no neuronal differentiation was observed. Interestingly, when demyelination was induced in the corpus callosum by a local injection of lysolecithin, increased number of cells derived from SVZ B1 cells and stimulated to migrate and proliferate by EGF infusion, differentiated into oligodendrocytes at the lesion site. This work indicates that EGF infusion can greatly expand the number of progenitors derived from the SVZ primary progenitors, which migrate and differentiate into oligodendroglial cells. This expanded population could be used for the repair of white matter lesions.

Keywords

Oligodendrogenesis; Subventricular zone; Epidermal growth factor; NG2 proteoglycan; adult neural stem cells; oligodendrocyte precursors; lysolecithin

Corresponding author: Arturo Alvarez-Buylla, Department of Neurosurgery and Institute for Regeneration Medicine., University of California, San Francisco. Box 0525, San Francisco, CA 94143, abuylla@stemcell.ucsf.edu.

Authors' contributions:

O. Gonzalez-Perez: Conception and design, collection and assembly of data, data analysis and interpretation, manuscript writing.
R. Romero-Rodriguez and M. Soriano-Navarro: Collection and assembly of data.
J.M. Garcia-Verdugo: Collection and assembly of data, data analysis and interpretation.
A. Alvarez-Buylla: Conception and design, financial support, manuscript writing.

Introduction

The subventricular zone (SVZ) is the largest source of progenitor cells in the adult mammalian brain. SVZ primary precursors correspond to a subpopulation of astroglial cells (type B1 cells) [1], which give rise to actively proliferating transit amplifying type C cells [2]. In rodents, most C cells generate neuroblasts (Type A cells) that migrate into the olfactory bulb via the rostral migratory stream (RMS) [3-6]. SVZ progenitors also generate a small number of oligodendrocytes that migrate into the corpus callosum, septum, striatum, and fimbria fornix [7-9].

In the presence of epidermal growth factor (EGF) and/or fibroblast growth factor (**FGF**), cultured SVZ progenitors self renew and upon removal of growth factors can generate neurons, astrocytes, and oligodendrocytes [10, 11]. *In vivo*, EGF, FGF2, or TGFα infusions result in a dramatic enlargement of the SVZ and increased migration of progenitor cells into the surrounding brain parenchyma [12-18]. Growth-factor infusions could therefore be useful in the amplification and mobilization of endogenous progenitor pools for brain repair. Earlier studies suggest that the majority of cells derived from the SVZ after EGF stimulation differentiate into astrocytes [14, 18]. Other studies suggest that *in vivo* EGFR signaling promotes SVZ progenitors to differentiate along the oligodendroglial lineage [16, 19] and one study reported that a small number of putative SVZ-derived cells in the striatum expresses neuronal markers [12]. These previous studies used BrdU or unspecific viral tracing analysis and cannot establish whether the newly generated cells after EGF infusion originated from SVZ primary progenitors or from other progenitors within or around the SVZ. We have previously shown that EGF can induce the proliferation and migration of cells derived from SVZ type B and C cells [13], but the fate of these cells was not established.

By specifically targeting the SVZ primary precursors, we show here that intraventricular infusion of EGF induces a dramatic expansion of cells derived from SVZ B1 cells. These cells upregulate Olig2 and migrate into the striatum, septum, and white matter tracts including the corpus callosum and fimbria fornix. Many of these cells differentiate into cells in the oligodendrocyte lineage. In addition, SVZ type-B cells also gave rise to a population of highly branched S100β+/GFAP+ cells and to a population of NG2+ oligodendrocyte progenitor cells (OPCs). Following induction of a demyelinating lesion in the corpus callosum, EGF-responsive cells derived from SVZ B1 cells migrated to the lesion site and differentiated into pre-myelinating and myelinating oligodendrocytes. Our results indicate that EGF signaling can greatly increase the number of SVZ-derived oligodendrocytes in the adult brain, and demonstrate that these new oligodendrocytes originate from SVZ B1 cells. Therefore, SVZ B1 progenitors can generate, under *in vivo* growth factor stimulation, a large number of cells that disperse and generate new OPCs and myelin-forming cells.

Materials and methods

Animal Care and Tissue Processing

All animal procedures followed the UC Committee on Animal Research guidelines. Adult CD-1 (Charles River, U.S.A.) and GFAP-tva (kind gift from E. Holland) mice were anesthetized by an intraperitoneal injection of 25-30μl/g body weight of 2.5% Avertin (2,2,2-tribromoethanol + tert-amyl alcohol, 1:1 w/v). Mice were sacrificed by an overdose of pentobarbital (100 mg/kg body weight) before transcardial perfusion. For light microscopy (n = 4 per group), mice were perfused with 4% paraformaldehyde (PFA) in 0.1M phosphate buffer (PB), and the brains were post-fixed overnight at 4°C in the same fixative. 30-μm thick coronal sections were cut with a vibratome. For electron microscopy (**EM**), mice were

sacrificed by intracardial perfusion with either 2% PFA / 0.5% glutaraldehyde for EM-immunocytochemistry or 2% PFA / 2.5% glutaraldehyde for conventional EM. For EM-immunocytochemistry (n = 3, per group), brains were post-fixed in the same fixative overnight at 4°C, cut coronally at 50 μm, and processed as described below. For conventional EM (n = 3, per group), 200 μm vibratome sections were post-fixed in 2% osmium for 2 h, rinsed, dehydrated, and embedded in Araldite (Durcupan, Fluka BioChemika, Ronkonkoma, NY). Sections (1.5 μm thick) were stained with 1% toluidine blue. To identify individual cell types, ultrathin (0.05 μm) sections were stained with lead citrate, and examined using a FEI Tecnai Spirit electron microscope. For freshly-dissociated cell staining, animals (n = 2 per group) were decapitated immediately after pump infusions and their brains immersed in ice-cold pipes buffer. Ipsilateral dorsal SVZ was dissected (1 mm length × 0.3 mm wide tissue piece from lateral wall of ventricle) (figure 4). SVZ was minced and incubated in 0.25% trypsin-EDTA solution at 37° C for 10 min. Then, trypsin was removed, fresh F-12 medium added and tissue triturated with a fire-polished pipette. The resulting cell suspension was placed, dried, and fixed with 3% of PFA onto glass slides. Staining was performed as described below.

Immunocytochemistry (ICC)

After blocking in 0.1M PBS containing 10% of normal goat serum for 1 h at room temperature, sections were incubated overnight at 4°C in primary antibodies diluted in blocking solution; 0.1% Triton-X was included for intracellular antigens. The following primary antibodies were used: mouse monoclonal to β-tubulin (1:500; Covance, Berkeley, CA), CNPase (1:250, Chemicon, Temecula, CA), GFAP (1:500, Chemicon), nestin (1:500, Chemicon), PSA-NCAM (1:1000, AbCys, France); rabbit polyclonal antibodies against S100β (1:500, Dako, Denmark), Olig2 (1:5000; kind gift from D. Rowitch), PDGFRα (1:50, Santa Cruz Immuno), NG2 (1:250; Chemicon), GFP (1:1000, Abcam, UK), and degraded Myelin Basic Protein (**dMBP**; 1:50, Chemicon). Polyclonal antibodies: guinea pig anti-doublecortin (1:1000, Chemicon), rat anti-MBP (1:250; Chemicon), and chicken anti-GFP (1:200; Aves Labs, Tigard, OR).

For fluorescent ICC (n = 4, per group), tissue sections were rinsed with 0.1 M PBS, incubated with the appropriate AlexaFluor conjugated secondary antibodies (all 1:500, Molecular Probes) in blocking solution for 1h at room temperature, and washed in PBS. For pre-embedding Olig2, GFP, and nestin ICC, sections were washed in PB, incubated in blocking solution with the appropriate biotinylated secondary antibody (1:400, Jackson Immuno) for 2 h at room temperature, incubated in ABC peroxidase kit (Vector) for 1 h and revealed with 0.03% diaminobenzidine and 0.01% H_2O_2. Controls in which primary antibodies were omitted resulted in no detectable staining. For imaging, a Zeiss LSM 510 laser scanning confocal microscope was used and optical 0.5 μm serial sections were obtained to co-localize fluorescent signals.

For pre-embedding EM-ICC (n = 3 per group), sections were washed in PB and incubated in blocking solution for 2 h at room temperature. Sections were then incubated in primary antibody: Olig2 (1:500), GFP (1:500), or Nestin (1:250) for 36 h at 4 °C, rinsed and incubated in biotinylated anti-rabbit IgG (1:400) overnight at 4°C, incubated in ABC peroxidase kit (Vector Laboratories, Burlingame, CA) for 2 h, and revealed with 0.03% diaminobenzidine (DAB) and 0.01% H_2O_2. Since DAB precipitates may be difficult to see under the EM, DAB+ cells are first identified and photographed by light microscopy on semi-thin 1-μm sections. Then, the same semi-thin sections are detached from the glass slides, flat-re-embedded and ultrathin sectioned to performed EM analysis.

For GFP pre-embedding immunogold (n = 3 per group), 50-μm vibratome sections in 0.1 M PBS + 25% saccharose were subjected to three 1-min freeze / thaw cycles and sequentially

incubated before araldite embedding in: 0.3% bovine serum albumin (BSA) / 0.1 M PBS for 1h at RT; chicken anti-GFP antibody (1:200; Aves Labs, Tigard, OR) in 0.3% BSA / 0.1M PBS for 60 h; 0.1M PBS, blocked in 0.5% BSA / 0.1% fish gelatin / 0.1 MPBS for 1 hr at RT; colloidal gold-conjugated anti-chicken IgG (0.8 nm particle diameter) diluted 1:50 in 0.1 M PBS / BSA-gelatin during 24 hr at RT; and the silver enhancement solution.

Retroviral Injections

Two days before pump infusions, RCAS-GFP retroviruses (100 nl; titer 3.07×10^7) were stereotaxically injected into adult GFAP-tva mice. Coordinates relative to Bregma and the surface of the brain (anterioposterior, mediolateral, and dorsoventral, respectively): 1, 1, 2.3; 0.5, 1.1, 1.7; 0, 1.4, 1.6 mm for the SVZ injections. To label non-SVZ astrocytes, we used: 0, 2.5, 2.5 and 0.5, 2.2, 2.5 mm for striatal injections (n = 3 per group); 1, 1.8, 1.25 mm for CC injections (n = 2 per group); 0, 2.8, 0.8 and 0.5, 2.5, 0.5 mm for cortical injections (n = 4 per group); and 0.5, 2.5, 0.1 for brain surface infusions (n = 2 per group).

EGF infusions

EGF (Upstate biotechnology) (400 ng/day) in vehicle (BSA / 0.9% saline) or vehicle alone was infused for 7 days with a mini-osmotic pump (Alzet, 1007D flow rate 0.5 ml/h). For infusions into the lateral ventricle, cannulas were implanted at 0 mm relative to Bregma, 1.1 mm lateral and 2.3 mm deep. For brain surface infusions, the dura mater was opened and the cannula placed at 0, 1.1, 0.5 mm (anterior, lateral, depth). Cannulas were removed on the seventh day and mice were sacrificed at different time points as indicated.

Demyelinating lesion

Demyelination was induced by injecting lysolecithin into corpus callosum as described previously [7, 8, 20]. RCAS-GFP was injected into the adult SVZ of GFAP-tva mice. Two days later, 0.5 μl of 1% lysolecithin (LPC; Sigma) in 0.9% NaCl was injected ipsilaterally into the corpus callosum at 1.1, 1, 1.5 mm (anterior, lateral, depth relative to bregma). EGF or vehicle was then infused onto the cortical surface, as described above. All animals (n = 3 per group) were sacrificed 30 days after EGF or vehicle pump removal.

Quantification

To quantify the number of Olig2+ cells, eight 30-μm sections that were 200-μm apart were randomly selected (n = 4 per group for 21 and 45 days post infusion; n = 3 per group for 90 and 180 d post infusion). The number of Olig2+ cells within 500 μm from the ependymal layer around the ventricle on the injected side was counted. A similar procedure was performed to quantify the number of DAPI+ cells that was used to calculate the cell density per mm^2. Double-labeled cells were counted in ten 30-μm sections, 120-μm apart (n = 3 - 4, per group). Only cells in which DAPI+ nuclei and overlapping marker expression was observed were counted as double-labeled. A similar procedure was used to determine the percentage of co-labeling in freshly-dissociated cells, where 200 randomly-selected cells per animal were counted and the percentage of co-labeled cells were calculated. Quantifications were made under an Olympus fluorescent microscope (AX70) using a 63X water-immersion objective. For demyelination experiments (n = 3, per group), CNPase+/GFP+ cells in corpus callosum in thirty 30-μm sections encompassing 500 μm rostrally and 500 μm caudally from the lysolecithin injection site were counted. To determine the demyelination volume (n = 3, per group), the whole brain was sectioned and sequential 15-μm coronal slices were collected every 60 μm. The demyelination lesion was calculated from the area of dMBP expression in the corpus callosum in serial sections using an image analyzer (Leica QWIN500I). Lesion area measurements were repeated three times for each brain. All data are expressed as means ± standard deviation. For comparisons of means between groups,

Student "*t*" test was used; $p < 0.05$ was considered significant. In all cases, quantifications were performed by a researcher blinded to group assignment.

Results

EGF generates a population of Olig2+Nestin+ invasive cells

EGF signaling induces an expansion of migrating progenitor cells around the SVZ [12-14]. To characterize these migrating cells, we infused EGF or vehicle into the lateral ventricles for 7 days, sacrificed the animals at the end of this treatment, and performed ICCs with neuronal and glial markers. Immediately after 7-day EGF infusions, there was a dramatic expansion of infiltrating cells around the SVZ. These infiltrating cells were negative to GFAP, vimentin, doublecortin, PSA-NCAM and S100β (data not shown). In contrast, there was a 9.6-fold increase in the number of Olig2+ cells around of the EGF-infused ventricles (1690 ± 558 cells per section; n = 4 animals, 8 sections each) as compared to the control-vehicle group (175 ± 19 cells per section; n = 4, 8 sections each, $P < 0.01$) (figure 1A-C). Here, we will refer to these cells as *EGF-induced progenitors* (**EIPs**). These infiltrating cells were not observed in saline-infused control animals (figure 1A, 2A-B), but many reactive astrocytes were observed close to the needle track, as in the EGF-infused group. We quantified the proportion of proliferating Olig2+ cells by injecting 50 mg/kg i.p. BrdU 1h before sacrifice. After a 7-d EGF infusion 3.9 % of the Olig2+ cells were BrdU+ (8/201 cells; n = 4) in saline-treated animals. In contrast, in the EGF-infused group 12.1 % of the Olig2+ cells were BrdU-labeled (110/908 cells; n = 4). The cellular infiltration around the ventricle resulted in a ~seven-fold increase in the density of cells (DAPI-stained nuclei) around the lateral ventricle (500 μm from the ependymal layer): The control group had 2.97×10^3 cells/mm^2 vs 2.08×10^4 cells/mm^2 in the EGF-infused group (n = 4 animals per group).

In accordance with previous studies [12, 14], after EGF infusions, we observed a dramatic expansion of nestin-expressing cells around the lateral ventricle. The distribution of nestin+ cells after 7-day EGF infusion was similar to that of Olig2+ cells (figure 1D-E). To determine if these nestin+ cells expressed Olig2, we performed double ICC and confocal analysis. The majority of, if not all, Olig2+ cells around the lateral ventricle appeared to co-express nestin (figure 1F). In order to confirm this observation, we used acutely dissociated cells from the periventricular region (figure 1G). The majority (92 ± 3 %) of Olig2+ cells co-expressed nestin (1337/1407 cells; n = 3). We also stained for NG2 and PDGFRα, which are expressed by OPCs, migrating and early differentiating oligodendrocytes [21, 22], but not by neuronal progeny [23, 24]. The number of NG2+ and PGDRFα+ cells was greatly increased around the ventricle of EGF-infused animals compared to controls (supplementary figure 1 A-D). These observations indicate that invading cells upon EGF infusion express markers of early neural progenitors or OPCs (nestin, Olig2, NG2 and PDGFRα) [25, 26].

To further define the EIP population we next studied their ultrastructure. Remarkably, in the SVZ of EGF-infused animals, type B cells were observed but type-C or -A cells were difficult to identify. Instead, we found large numbers of cells in the SVZ and striatum with a unique set of ultrastructural characteristics (figure 2A-F): irregular cytoplasmic profiles, characteristic electrondense cytosolic inclusions, and large nuclear invaginations. Their nuclei were voluminous and irregular, with heterogeneous chromatin and prominent nucleoli. A number of dictiosomes, abundant ribosomes, profuse rough endoplasm reticuli and mitochondria were also observed, but no obvious polarization of organelles was found. Electrondense intercellular junctions, intercellular spaces, endocytic vesicles and mitoses were also frequently found among these invading cells (figure 2D-F). These cells were usually elongated and had a migratory morphology. Pre-embedding ICC analysis showed that these cells (with distinctive ultrastructural characteristics) expressed Olig2 in their

nuclei (figure 2G-J), confirming that they corresponded to the population of infiltrating cells characterized above by light microscopy. The EIPs were tightly associated to blood vessels in the vicinity of the SVZ, in the corpus callosum, striatum, and septum (figure 2B-C, G-J). However, EIPs were not in direct contact with the endothelial cells but separated from these cells by thin astrocytic processes (supplementary figure 1). These results indicate that EIPs cells have unique ultrastructural characteristics different from those of normal SVZ progenitors and express nestin and Olig2.

EIPs are derived from SVZ B1 cells and differentiate into oligodendrocyte precursors

To investigate whether the Olig2+ EIPs were derived from the SVZ B1 cells, we used GFAP-tva mice [27] and the avian leukosis retrovirus expressing the reporter gene green fluorescent protein (**RCAS-GFP**). In these mice, this vector selectively infects dividing GFAP+ SVZ astrocytes cells in the SVZ allowing permanent labeling of their progeny [2, 13]. RCAS-GFP was injected into the mouse SVZ of GFAP-tva mice. Two days later, EGF or vehicle was infused into the lateral ventricle for 7 days. Immediately after the 7-day EGF infusions, the animals were sacrificed and many GFP+ cells were observed around the ventricle (figure 3A-B). These GFP+ cells had identical ultrastructure as the EIPs described above (figure 3C). Since the RCAS-GFP labeling revealed the processes and shape of the EIPs in more detail, we performed 3-D Z-stack confocal reconstructions of 36 individual cells. Two general morphologies were observed (figure 3D): 1) Simple, unipolar or bipolar cells. These cells were found preferentially close to the lateral ventricle and were frequently associated to blood vessels or axonal tracts. Their location and morphology suggest that these cells correspond to actively migrating EGF-responsive cells. These cells had a dominant leading process with numerous thin ramifications. In about half of the cells, a smaller trailing process was observed. 2) Complex or multipolar cells with three or more primary processes and highly ramified branches. These cells were found throughout the region of invasion. To establish whether the simple and complex cells also had different ultrastructural characteristics, we performed 3D reconstructions by EM (n = 12 cells) (figure 3E). Interestingly, the EIPs found close to the lateral ventricle had less cellular processes, ribosomes, and mitochondria. These cells were also smaller (5 - 10 μm) than the cells found in the striatum or septum (15 - 20 μm), which contained abundant electrondense cytosolic inclusions, ribosomes, rough-endoplasm reticuli, and large nuclear invaginations. This more complex morphology suggests that these cells are not migratory; however, we do not know how dynamic the processes on these cells are and whether complex cells could revert to a migratory phenotype.

To establish the phenotype of the RCAS-GFP-labeled EIPs, we performed double ICC and confocal analysis. This analysis confirms that most of the GFP+ cells co-expressed Olig2 (figure 4A). Interestingly, a high percentage of them also co-expressed NG2 or PDGFRα (figure 4B-C). To further verify the double-labeling between GFP and Olig2, NG2, or PDGFRα, and to determine the percent of double-labeled cells, we dissociated the cells isolated from periventricular regions immediately after the 7-d EGF infusion: 97 ± 1 % (205/211 cells; n = 2) of GFP cells co-expressed Olig2; 84 ± 17 % (273/323 cells; n = 2) co-expressed PDGFRα, and 87 ± 14 % (201/227 cells; n = 2) co-expressed NG2. No PSA-NCAM+ or doublecortin+ cells were observed in the SVZ of the EGF infused animals (data not shown). The above results strongly suggest that the EIPs, derived from the type B SVZ cells, express markers related to oligodendrocyte precursors.

To analyze whether non-SVZ dividing astrocytes from other brain regions may give rise to Olig2+ EIPs, we infused EGF into the lateral ventricle and injected RCAS-GFP in three different locations: cortex (n = 4), corpus callosum (n = 2), striatum (n = 3), and brain surface (n = 2) (supplementary figure 2). After 7-day EGF infusions, only a small population

of GFAP+ astrocytes was found labeled close to the injection site at cortex, corpus callosum, and striatum (supplementary figure 2), but no GFP+ cells were observed to be infiltrating the parenchyma as seen when the RCAS virus is targeted to the SVZ. No GFP+ cells were observed when virus was injected onto the brain surface. These results confirm that the SVZ astrocytes (SVZ B1 cells) are the most important source of the Olig2+NG2+PDGFRα+ cells that appear in the parenchyma after EGF infusion.

EIPs differentiate along the oligodendrocyte lineage

We next investigated the long-term fate of the EGF-invaders in the brain. In order to label the cell progenitors derived from the SVZ astrocytes, we used GFAP-tva mice labeled with RCAS-GFP as described above. After 7-day intraventricular infusions of EGF, the micro-osmotic pumps were removed and animals were allowed to survive for 21 days (n = 5). At this time, many more labeled cells were found in the corpus callosum, septum, striatum, cortex, and fimbria fornix regions as compared to controls (figure 5A-B). The cells fond in cortex were not only distributed along the needle track, but also found as far as 800-1000 μm from the SVZ or the needle track. We analyzed the cells found in the corpus callosum in detail and found that they had round or elongated cell somas. Clusters of 3-4 elongated GFP + cells were frequently observed to align with callosal fiber tracts (figure 5C-D). To reveal the morphology of these cells in more detail, we performed serial confocal analysis of 10-15 optical sections (0.75-1 μm thick) in 68 cells. About half of these cells had morphological characteristics of pre-myelinating and myelinating oligodendrocytes. In addition, transitional forms between the migrating morphology and the pre-myelinating oligodendrocytes were also observed [7, 28, 29](figure 5E-G). Pre-myelinating oligodendrocytes were characterized by their multiple radial processes and thin bushy branches (figure 5E), while myelinating oligodendrocytes had the typical elongated sheaths aligned with fiber tracts (figure 5F). Oligodendrocytes were also observed in some myelinated tracts in the striatum, cortex, and septum (data not shown). We also sacrificed animals at 45 (n = 4), 90 (n = 3), and 180 (n = 3) days after removal of EGF infusion. Similar morphologies were observed at these longer survival times suggesting that SVZ cells invade the brain in response to EGF and differentiate into mature oligodendrocytes. Oligodendrocytes in the corpus callosum and fimbria were also observed in saline controls (n = 4, for 21 d and 45 d; n = 3, for 90 and 180 d after pump withdrawal), but their numbers were small as compared to the EGF-infused animals. In the saline-infused animals, GFP+ oligodendrocytes were very rare in the septum and striatum, and were not observed in cortex (supplementary figure 3).

To further establish the identity of cells derived from EIPs, we counterstained sections with different oligodendrocyte lineage markers. The precursor markers included Olig2 [30, 31], anti-NG2 [21, 22], and PDGFRα [32]. The pre-myelinating oligodendrocytes markers included CNPase [33] and β-IV tubulin [34], and the myelinating oligodendrocytes included MBP [29]. We also stained sections for S100β, which is typically associated with parenchymal astrocytes [35], but has been recently associated with oligodendrocyte precursors [36, 37]. Most of the GFP+ cells in the corpus callosum expressed oligodendrocyte markers (figure 5H-N). For quantification purposes (table 1), we selected markers that delineate cell bodies and/or nuclei, such as: CNPase, Olig2, S100β, and NG2. We found a 200-400% increase in the number of GFP-labeled cells that express these markers at 21, 45, 90, and 180 days after EGF infusion compared to controls (table 1). These findings indicate that the EGF-expanded cells, which are derived from SVZ B1 cells, invade the corpus callosum and fimbria. They then largely differentiate into oligodendrocyte lineage. The increased number of S100β+GFP+ cells in corpus callosum after the EGF infusion was comparable to that observed with other oligodendrocyte markers. Interestingly, within the striatum and septum at 21, 45, 90, and 180 days after EGF infusion, SVZ B1 cells gave rise not only to NG2+ cells but also to a subpopulation of highly branched S100β+/

GFAP+/NG2- cells (supplementary figure 3). The branched morphology and low expression of GFAP [38] may indicate that the SVZ expanded population under EGF has the ability to differentiate into parenchymal astrocytes. However, these unique cells also express S100β, which could indicate that they are part of the oligodendrocyte lineage (see discussion) [36, 37].

A previous study suggests that a small subpopulation of SVZ progenitors, which migrate into the striatum after EGF infusion, differentiate into neurons [12]. Interestingly, at all ages after EGF infusions, short chains of 4-7 GFP+ cells that stained positively for doublecortin and PSA-NCAM were observed from 20 to 50 μm deep from the SVZ in the striatum and septum (supplementary figure 4). These chains were never observed in control animals. In order to test whether these cells differentiate into mature neurons, we stained sections with the marker NeuN at 21, 45, 90, and 180 days (3 - 5 animals per age group) after EGF withdrawal. We found no evidence of GFP+ cells differentiate into neurons in the striatum, septum, or cortex, even at longer survival times. Cells in these chains may die or rejoin the network of pathways for chain migration in the SVZ. The above observations indicate that after withdrawal of EGF, EIPs differentiate into NG2+ OPCs, mature oligodendrocytes, and a population of S100β+/GFAP+ cells.

EGF-expanded oligodendrocytes derived from SVZ B1 cells promote remyelination

We next investigated whether cells derived from SVZ type B cells can contribute to increase the number of oligodendrocytes into demyelinating lesions after EGF infusion. SVZ astrocytes were labeled by injecting RCAS-GFP into the SVZ of adult GFAP-tva mice. Two days later, lysolecithin or vehicle was ipsilaterally injected into the corpus callosum. To avoid an additional injury in the corpus callosum, the cannula for EGF or vehicle infusion was placed onto the brain surface. We found that EGF infusion onto the brain surface expands the number of Olig+ cells that invade surrounding brain parenchyma as seen with intraventricular infusions (supplementary figure 5). The cells that leave the SVZ expressed Olig2 and had the same morphological characteristics of the EIPs expanded by intraventricular infusions following EGF-infusion onto the brain surface. Animals were sacrificed at 14 and 28 days post-lysolecithin injection (**DPL**). At 14 DPL, we found a 2.1-fold increase in the number of GFP+/CNPase+ cells in the corpus callosum of EGF-infused animals (181 ± 36, n = 3) compared with the control-vehicle group (84 ± 19, n = 3; $P < 0.05$). At 28 DPL, we found a 2.6-fold increase in the number of GFP+/CNPase+ cells in the corpus callosum of EGF-infused brains (251 ± 36 cells, n = 3) versus the control-vehicle group (94 ± 35 cells, n = 3; $P < 0.01$) (figure 6A-B, D). These GFP+ cells in the lesion site contacting neurofilaments had the morphology and expressed oligodendrocyte markers (CNPase, MBP, S100β) (figure 6 C-G). To quantify the effect of EGF on remyelination, we performed immunohistochemistry for degraded-myelin basic protein (**dMBP**) at 14 and 28 DPL and calculated the volume of the demyelinating lesion in the corpus callosum (n = 3 per group) (figure 6 H-J). In both cases, EGF-treated animals had significantly smaller lesion volumes (at 14 DPL = 0.55 ± 0.04 mm^3, and at 28 DPL = 0.23 ± 0.05 mm^3) compared to controls (at 14 DPL = 0.33 ± 0.08 mm^3, and at 28 DPL = 0.4 ± 0.04 mm^3; $P < 0.05$, Student “t” test). These findings indicate that EGF increases the number of oligodendrocytes derived from SVZ B1 cells that contribute to remyelination after a demyelinating lesion to the corpus callosum.

Discussion

Here, we show that the majority of cells derived from SVZ B1 cells after EGF infusion leave the SVZ and migrate along axonal tracts and blood vessels, express Olig2 and other OPC markers, and differentiate into non-myelinating and myelinating oligodendrocytes. EGF

induces proliferation and migration of the SVZ progenitors in embryonic, early postnatal, and adult brain [12, 14, 17, 39-41]. Consistently, our present results indicate that the EGF infusion into adult brain induces expansion of highly-migratory SVZ progenitors. Interestingly, the majority of these EGF-expanded progenitors express Olig2. This is in sharp contrast to the normal conditions in which only a small subpopulation of SVZ B1 and C cells express Olig2 [7, 25, 42]. Olig2 is essential for the proliferation and differentiation of oligodendrocyte precursors [31, 43-46]. Olig2 expressing progenitors also give rise to motor neurons [44, 47, 48], astrocytes, and ependymal cells [26, 49]. Even though Olig2 expression has been reported in OPCs and mature oligodendrocytes [50, 51], it is not possible to conclude that EIPs are committed to the oligodendroglial lineage based on the expression of Olig2 alone.

Interestingly, Olig2 overexpression has also been reported in glioma-like growths induced by PDGFα [52] and in multiple types of brain tumors [50, 53]. Similar to PDGFα, Olig2 is required for neurosphere formation and tumor growth [54]. Interestingly, unlike PDGFα, EGF infusion up-regulates Olig2 expression, but did not generate glioma-like masses next to the SVZ. Instead, EGF produced highly-motile Olig2+ cells that infiltrate the brain parenchyma along blood vessels, as well as myelinated and non-myelinated axonal tracts, which is a behavior comparable to that of invading brain tumor cells [50, 55, 56]. Aberrant EGF signaling has been implicated in glioma progression [55, 56]. Long-lasting constitutive EGF signaling has also been found to lead to diffuse hyperplasia of early glial progenitors in the white matter without differentiation into mature oligodendrocytes [57]. Other studies have reported polyp-like formation after a long-term EGF infusion [14] or transplantation of EGF-treated neural progenitors [58]. However, none of our animals, including some that survived for 180 days after termination of EGF infusions, had tumors. Although EGFR mutations confer enhanced tumorigenic behavior, the evidence indicates that EGF signaling alone is not enough to produce tumors [55, 59]. Our data indicate that cell proliferation and infiltration cease soon after termination of EGF infusion, and most of the cells differentiate into cells in the oligodendroglial lineage.

While previous studies have followed the differentiation of EGF-expanded populations from the SVZ [12, 14, 18], none have traced the differentiation of cells derived from the primary SVZ progenitors. Furthermore, since EGF may induce proliferation of SVZ progenitors as well as other precursors outside of the SVZ, it was important to establish the fate of cells derived from the SVZ B1 cells. Towards this end, we used GFAP-tva mice in which GFAP-expressing SVZ cells can be specifically infected with RCAS retrovirus carrying a GFP reporter gene [2, 13, 27]. In all our experiments, RCAS labeling was done before EGF-pump implantation to avoid a potential EGF-induced expression of tva receptors in other cells. We found that the EGF-expanded cells that invade the brain parenchyma were derived from the SVZ B1 cells. Interestingly, in addition to Olig2, these EGF-expanded population also expressed PDGFRα and NG2 [60], which are markers associated with oligodendrocyte lineage [24, 61-63].

Most of the GFP-labeled cells (from 21 to 180 days) in the corpus callosum and fimbria not only had the morphology, but also expressed markers consistent for cells in the oligodendrocyte lineage. In addition to oligodendrocytes, we also found that the EIPs gave rise to a population of S100β+ cells. These cells expressed low levels of GFAP and had a “bushy” morphology similar to that of protoplasmic astrocytes. This is consistent with previous work suggesting that intracerebral infusion of EGF results in the generation of astrocytes [12, 14]. Since most, if not all, of the EGF-responsive cells expressed Olig2, these astrocyte-like cells were likely derived from Olig2-expressing cells. This is consistent with recent work suggesting that Olig2-expressing precursors also can generate astrocytes in addition to oligodendrocytes [26]. However, S100β, which is typically identified as a marker

of astrocytes [35], has recently been found in the oligodendroglial lineage [36, 37]. Therefore, the S100β+ "astrocytes" we observed in gray matter brain regions may also correspond to cells in the OPC lineage. The precise nature of GFAP+/S100β+ cell population remains unresolved. Previous studies reported that a small subpopulation of EGF-expanded SVZ cells differentiates into neurons [12]. We did not observe neuronal differentiation in the striatum, septum, and cortex at any of the studied survival times.

Under normal conditions, the production of oligodendrocytes from SVZ B1 stem cells is low compared to neuronal generation [7]. SVZ oligodendrocyte production increases in response to demyelination [7-9, 64], yet cell recruitment into the lesion is not extensive. The present results show that EGF infusion can significantly increase the number of oligodendrocytes derived from B1 SVZ cells, which contribute to myelin repair. This is consistent with recent work showing that EGFR signaling significantly increases the number of oligodendrocytes derived from the SVZ and stimulates migration and remyelination [16]. Developmental studies indicate that changes in EGFR expression onto cell membrane can influence cell fate and its overexpression pushes cells into glial lineage at the expense of neuron formation [39, 41, 65]. However, further studies are necessary to establish whether asymmetric distribution of EGFR during mitosis is responsible of glial fate inductions in adult brain, as reported in developmental studies [66]. In the adult brain, mature oligodendrocytes are not only produced from the SVZ [7-9], but also from local NG2-expressing OPCs [21, 67]. We found that after EGF stimulation, NG2+ cells in the white and gray matter derived from SVZ B1 cells. NG2+ cells also referred as OPCs, polidendrocytes [61], NG2-expressing glia [63], and synantocytes [68], are likely functionally diverse. Subsets of NG2-expressing cells express AMPA (α-amino-3-hydroxy-5-methyl isoxazole propionic acid) receptors and participate in glutamatergic synaptic signaling in the hippocampus [69], corpus callosum [70] and cortex [71]. We do not know if the population of NG2-expressing cells that are derived by EGF infusions from SVZ type B cells is homogeneous or if different subpopulations of NG2-expressing glia can be generated by this method. Interestingly, synantocytes or polidendrocytes have been implicated in brain scar formation and response to demyelination [28, 72, 73]. Recent evidence has also shown that erythropoietin/EGF-amplified cells from the SVZ may also contribute to functional cortical repair [74]. The above suggests that, in addition to their classical function as local OPCs, the EGF-derived NG2+ populations could play important roles in brain repair.

Remyelination has been observed following neural stem cell transplantation into experimental demyelination models [75, 76]. However, one limitation of this approach is delayed rejection to grafted precursors [77, 78]. Recruitment of new OPCs by stimulation of endogenous precursors circumvents immune rejection [79]. The present work shows that EGF stimulates the endogenous SVZ progenitors to differentiate into myelin-forming cells. Interestingly, a local proliferative response has been described in the human SVZ of patients suffering from multiple sclerosis [80] suggesting that local periventricular oligodendrocyte progenitors may exist in the adult human brain.

Conclusions/Summary

Taken together our results indicate that EGF infusion in the adult mouse brain significantly increases the number of progenitor cells derived from SVZ stem cells. EGF stimulates these progenitors to migrate long distances in the adult brain [13, 16, 17] [present results], which results in massive infiltration into regions that usually receive few new cells from the SVZ (corpus callosum, fimbria-fornix, striatum, septum, and cortex). Most of the amplified cells differentiate along the oligodendrocyte lineage, and contribute to the repair of demyelinating lesions. Effective precursor infiltration and differentiation of OPCs into myelinating oligodendrocytes are considered crucial steps for the development of new cell repair

strategies for demyelinating diseases [81]. Our data indicate that the lineage of cells derived from stem cells in the largest germinal layer of the adult brain can be manipulated by infusion of growth factors to significantly increase the formation of oligodendrocytes.

Supplementary Material

Refer to Web version on PubMed Central for supplementary material.

Acknowledgments

This work was supported by NIH grant HD 32116, the Goldhirsh Foundation, and the John G. Bowes research fund. O.G-P. was supported by FRABA grant (No. 554/08). A.A-B holds the Heather and Melanie Muss Endowed Chair. J.M.G-V was supported by CIBERNED and Red de Terapia Celular. We would like to thank David Rowitch for providing Olig2 antibody, Magdalena Gotz for the RCAS-GFP DNA construct, Eric Holland for the GFAP-tva mice, and Sonia Luquin for her technical support. We are also grateful to Thuhien Nguyen, Cynthia Yaschine and Kaisorn Chaichana for the editorial comments on the MS.

REFERENCES

1. Mirzadeh Z, Merkle FT, Soriano-Navarro M, et al. Neural stem cells confer unique pinwheel architecture to the ventricular surface in neurogenic regions of the adult brain. Cell stem cell. 2008; 3:265–278. [PubMed: 18786414]
2. Doetsch F, Caille I, Lim DA, et al. Subventricular Zone Astrocytes Are Neural Stem Cells in the Adult mammalian Brain. Cell. 1999; 97:1–20. [PubMed: 10199395]
3. Altman J. Autoradiographic and Histological Studies of Postnatal Neurogenesis. IV. Cell Proliferation and Migration in The Anterior Forebrain, With Special Reference to Persisting Neurogenesis in The Olfactory Bulb. J Comp Neurol. 1969; 137:433–458. [PubMed: 5361244]
4. Lois C, Alvarez-Buylla A. Long-distance neuronal migration in the adult mammalian brain. Science. 1994; 264:1145–1148. [PubMed: 8178174]
5. Doetsch F, Alvarez-Buylla A. Network of tangential pathways for neuronal migration in adult mammalian brain. Proc Natl Acad Sci USA. 1996; 93:14895–14900. [PubMed: 8962152]
6. Luskin MB, Parnavelas JG, Barfield JA. Neurons, astrocytes, and oligodendrocytes of the rat cerebral cortex originate from separate progenitor cells: An ultrastructural analysis of clonally related cells. J.Neurosci. 1993; 13:1730–1750. [PubMed: 8463848]
7. Menn B, Garcia-Verdugo JM, Yaschine C, et al. Origin of oligodendrocytes in the subventricular zone of the adult brain. J Neurosci. 2006; 26:7907–7918. [PubMed: 16870736]
8. Nait-Oumesmar B, Decker L, Lachapelle F, et al. Progenitor cells of the adult mouse subventricular zone proliferate, migrate and differentiate into oligodendrocytes after demyelination. Eur J Neurosci. 1999; 11:4357–4366. [PubMed: 10594662]
9. Picard-Riera N, Decker L, Delarasse C, et al. Experimental autoimmune encephalomyelitis mobilizes neural progenitors from the subventricular zone to undergo oligodendrogenesis in adult mice. Proc Natl Acad Sci U S A. 2002; 99:13211–13216. [PubMed: 12235363]
10. Reynolds B, Weiss S. Generation of neurons and astrocytes from isolated cells of the adult mammalian central nervous system. Science. 1992; 255:1707–1710. [PubMed: 1553558]
11. Vescovi AL, Reynolds BA, Fraser DD, et al. bFGF regulates the proliferative fate of unipotent (neuronal) and bipotent (neuronal/astroglial) EGF-generated CNS progenitor cells. Neuron. 1993; 11:951–966. [PubMed: 8240816]
12. Craig CG, Tropepe V, Morshead CM, et al. *In vivo* growth factor expansion of endogenous subependymal neural precursor cell populations in the adult mouse brain. J.Neurosci. 1996; 16:2649–2658. [PubMed: 8786441]
13. Doetsch F, Petreanu L, Caille I, et al. EGF converts transit-amplifying neurogenic precursors in the adult brain into multipotent stem cells. Neuron. 2002; 36:1021–1034. [PubMed: 12495619]
14. Kuhn HG, Winkler J, Kempermann G, et al. Epidermal growth factor and fibroblast growth factor-2 have different effects on neural progenitors in the adult rat brain. J.Neurosci. 1997; 17:5820–5829. [PubMed: 9221780]

15. Fallon J, Reid S, Kinyamu R, et al. In vivo induction of massive proliferation, directed migration, and differentiation of neural cells in the adult mammalian brain. Proc Natl Acad Sci U S A. 2000; 97:14686–14691. [PubMed: 11121069]
16. Aguirre A, Dupree JL, Mangin JM, et al. A functional role for EGFR signaling in myelination and remyelination. Nat Neurosci. 2007; 10:990–1002. [PubMed: 17618276]
17. Aguirre A, Rizvi TA, Ratner N, et al. Overexpression of the epidermal growth factor receptor confers migratory properties to nonmigratory postnatal neural progenitors. J Neurosci. 2005; 25:11092–11106. [PubMed: 16319309]
18. Cantarella C, Cayre M, Magalon K, et al. Intranasal HB-EGF administration favors adult SVZ cell mobilization to demyelinated lesions in mouse corpus callosum. Dev Neurobiol. 2008; 68:223–236. [PubMed: 18000828]
19. Hammang JP, Archer DR, Duncan ID. Myelination following transplantation of EGF-responsive neural stem cells into a myelin-deficient environment. Exp Neurol. 1997; 147:84–95. [PubMed: 9294405]
20. Gensert JM, Goldman JE. In vivo characterization of endogenous proliferating cells in adult rat subcortical white matter. Glia. 1996; 17:39–51. [PubMed: 8723841]
21. Stallcup WB, Beasley L. Bipotential glial precursor cells of the optic nerve express the NG2 proteoglycan. J Neurosci. 1987; 7:2737–2744. [PubMed: 3305800]
22. Reynolds R, Hardy R. Oligodendroglial progenitors labeled with the O4 antibody persist in the adult rat cerebral cortex in vivo. J Neurosci Res. 1997; 47:455–470. [PubMed: 9067855]
23. Pringle NP, Richardson WD. A singularity of PDGF alpha-receptor expression in the dorsoventral axis of the neural tube may define the origin of the oligodendrocyte lineage. Development. 1993; 117:525–533. [PubMed: 8330523]
24. Nishiyama A, Lin XH, Giese N, et al. Co-localization of NG2 proteoglycan and PDGF alpha-receptor on O2A progenitor cells in the developing rat brain. J Neurosci Res. 1996; 43:299–314. [PubMed: 8714519]
25. Hack MA, Saghatelyan A, de Chevigny A, et al. Neuronal fate determinants of adult olfactory bulb neurogenesis. Nat Neurosci. 2005
26. Marshall CA, Novitch BG, Goldman JE. Olig2 directs astrocyte and oligodendrocyte formation in postnatal subventricular zone cells. J Neurosci. 2005; 25:7289–7298. [PubMed: 16093378]
27. Holland EC, Varmus HE. Basic fibroblast growth factor induces cell migration and proliferation after glia-specific gene transfer in mice. Proc.Natl.Acad.Sci.USA. 1998; 95:1218–1223. [PubMed: 9448312]
28. Butt, AM. Structure and function of oligodendrocytes. In: Ketternmann HaR, BR., editor. Second ed. Oxford University Press; New York: 2005. p. 36-47.
29. Pfeiffer SE, Warrington AE, Bansal R. The oligodendrocyte and its many cellular processes. Trends Cell Biol. 1993; 3:191–197. [PubMed: 14731493]
30. Takebayashi H, Yoshida S, Sugimori M, et al. Dynamic expression of basic helix-loop-helix Olig family members: implication of Olig2 in neuron and oligodendrocyte differentiation and identification of a new member, Olig3. Mech Dev. 2000; 99:143–148. [PubMed: 11091082]
31. Zhou Q, Wang S, Anderson DJ. Identification of a novel family of oligodendrocyte lineage-specific basic helix-loop-helix transcription factors. Neuron. 2000; 25:331–343. [PubMed: 10719889]
32. McKinnon RD, Matsui T, Dubois-Dalcq M, et al. FGF modulates the PDGF-driven pathway of oligodendrocyte development. Neuron. 1990; 5:603–614. [PubMed: 2171589]
33. Vogel US, Reynolds R, Thompson RJ, et al. Expression of the 2′,3′-cyclic nucleotide 3′-phosphohydrolase gene and immunoreactive protein in oligodendrocytes as revealed by in situ hybridization and immunofluorescence. Glia. 1988; 1:184–190. [PubMed: 2852171]
34. Terada N, Kidd GJ, Kinter M, et al. Beta IV tubulin is selectively expressed by oligodendrocytes in the central nervous system. Glia. 2005; 50:212–222. [PubMed: 15712210]
35. Reeves RH, Yao J, Crowley MR, et al. Astrocytosis and axonal proliferation in the hippocampus of S100b transgenic mice. Proc Natl Acad Sci U S A. 1994; 91:5359–5363. [PubMed: 8202493]

36. Deloulme JC, Raponi E, Gentil BJ, et al. Nuclear expression of S100B in oligodendrocyte progenitor cells correlates with differentiation toward the oligodendroglial lineage and modulates oligodendrocytes maturation. Mol Cell Neurosci. 2004; 27:453–465. [PubMed: 15555923]
37. Hachem S, Aguirre A, Vives V, et al. Spatial and temporal expression of S100B in cells ofoligodendrocyte lineage. Glia. 2005; 51:81–97. [PubMed: 15782413]
38. Brenner M, Kisseberth WC, Su Y, et al. GFAP promoter directs astrocyte-specific expression in transgenic mice. J Neurosci. 1994; 14:1030–1037. [PubMed: 8120611]
39. Burrows RC, Wancio D, Levitt P, et al. Response diversity and the timing of progenitor cell maturation are regulated by developmental changes in EGFR expression in the cortex. Neuron. 1997; 19:251–267. [PubMed: 9292717]
40. Ciccolini F, Svendsen CN. Fibroblast growth factor 2 (FGF-2) promotes acquisition of epidermal growth factor (EGF) responsiveness in mouse striatal precursor cells: identification of neural precursors responding to both EGF and FGF-2. J.Neurosci. 1998; 18:7869–7880. [PubMed: 9742155]
41. Caric D, Raphael H, Viti J, et al. EGFRs mediate chemotactic migration in the developing telencephalon. Development. 2001; 128:4203–4216. [PubMed: 11684657]
42. Hack MA, Sugimori M, Lundberg C, et al. Regionalization and fate specification in neurospheres: the role of Olig2 and Pax6. Mol Cell Neurosci. 2004; 25:664–678. [PubMed: 15080895]
43. Rowitch DH, Lu QR, Kessaris N, et al. An ‘oligarchy’ rules neural development. Trends Neurosci. 2002; 25:417–422. [PubMed: 12127759]
44. Takebayashi H, Nabeshima Y, Yoshida S, et al. The basic helix-loop-helix factor olig2 is essential for the development of motoneuron and oligodendrocyte lineages. Curr Biol. 2002; 12:1157–1163. [PubMed: 12121626]
45. Lu QR, Yuk D, Alberta JA, et al. Sonic hedgehog--regulated oligodendrocyte lineage genes encoding bHLH proteins in the mammalian central nervous system. Neuron. 2000; 25:317–329. [PubMed: 10719888]
46. Copray S, Balasubramaniyan V, Levenga J, et al. Olig2 overexpression induces the in vitro differentiation of neural stem cells into mature oligodendrocytes. Stem Cells. 2006; 24:1001–1010. [PubMed: 16253982]
47. Lu QR, Sun T, Zhu Z, et al. Common developmental requirement for Olig function indicates a motor neuron/oligodendrocyte connection. Cell. 2002; 109:75–86. [PubMed: 11955448]
48. Zhou Q, Choi G, Anderson DJ. The bHLH transcription factor Olig2 promotes oligodendrocyte differentiation in collaboration with Nkx2.2. Neuron. 2001; 31:791–807. [PubMed: 11567617]
49. Masahira N, Takebayashi H, Ono K, et al. Olig2-positive progenitors in the embryonic spinal cord give rise not only to motoneurons and oligodendrocytes, but also to a subset of astrocytes and ependymal cells. Dev Biol. 2006
50. Ligon KL, Alberta JA, Kho AT, et al. The oligodendroglial lineage marker OLIG2 is universally expressed in diffuse gliomas. J Neuropathol Exp Neurol. 2004; 63:499–509. [PubMed: 15198128]
51. Rowitch DH. Glial specification in the vertebrate neural tube. Nat Rev Neurosci. 2004; 5:409–419. [PubMed: 15100723]
52. Jackson EL, Garcia-Verdugo JM, Gil-Perotin S, et al. PDGFR alpha-positive B cells are neural stem cells in the adult SVZ that form glioma-like growths in response to increased PDGF signaling. Neuron. 2006; 51:187–199. [PubMed: 16846854]
53. Marie Y, Sanson M, Mokhtari K, et al. OLIG2 as a specific marker of oligodendroglial tumour cells. Lancet. 2001; 358:298–300. [PubMed: 11498220]
54. Ligon KL, Huillard E, Mehta S, et al. Olig2-regulated lineage-restricted pathway controls replication competence in neural stem cells and malignant glioma. Neuron. 2007; 53:503–517. [PubMed: 17296553]
55. Bachoo RM, Maher EA, Ligon KL, et al. Epidermal growth factor receptor and Ink4a/Arf. Convergent mechanisms governing terminal differentiation and transformation along the neural stem cell to astrocyte axis. Cancer Cell. 2002; 1:269–277. [PubMed: 12086863]
56. Maher EA, Furnari FB, Bachoo RM, et al. Malignant glioma: genetics and biology of a grave matter. Genes Dev. 2001; 15:1311–1333. [PubMed: 11390353]

57. Ivkovic S, Canoll P, Goldman JE. Constitutive EGFR signaling in oligodendrocyte progenitors leads to diffuse hyperplasia in postnatal white matter. J Neurosci. 2008; 28:914–922. [PubMed: 18216199]
58. Lachapelle F, Avellana-Adalid V, Nait-Oumesmar B, et al. Fibroblast growth factor-2 (FGF-2) and platelet-derived growth factor AB (PDGF AB) promote adult SVZ-derived oligodendrogenesis in vivo. Mol Cell Neurosci. 2002; 20:390–403. [PubMed: 12139917]
59. Holland EC, Hively WP, DePinho R, et al. Constitutively active epidermal growth factor receptor cooperates with disruption of G1 cell-cycle arrest pathways to induce glioma-like lesions in mice. Genes & Development. 1998; 12:3675–3685. [PubMed: 9851974]
60. Stegmuller J, Schneider S, Hellwig A, et al. AN2, the mouse homologue of NG2, is a surface antigen on glial precursor cells implicated in control of cell migration. J Neurocytol. 2002; 31:497–505. [PubMed: 14501219]
61. Nishiyama A. Polydendrocytes: NG2 cells with many roles in development and repair of the CNS. Neuroscientist. 2007; 13:62–76. [PubMed: 17229976]
62. Ligon KL, Kesari S, Kitada M, et al. Development of NG2 neural progenitor cells requires Olig gene function. Proc Natl Acad Sci U S A. 2006; 103:7853–7858. [PubMed: 16682644]
63. Horner PJ, Thallmair M, Gage FH. Defining the NG2-expressing cell of the adult CNS. J Neurocytol. 2002; 31:469–480. [PubMed: 14501217]
64. Petratos S, Gonzales MF, Azari MF, et al. Expression of the low-affinity neurotrophin receptor, p75(NTR), is upregulated by oligodendroglial progenitors adjacent to the subventricular zone in response to demyelination. Glia. 2004; 48:64–75. [PubMed: 15326616]
65. Viti J, Feathers A, Phillips J, et al. Epidermal growth factor receptors control competence to interpret leukemia inhibitory factor as an astrocyte inducer in developing cortex. J Neurosci. 2003; 23:3385–3393. [PubMed: 12716946]
66. Sun Y, Goderie SK, Temple S. Asymmetric distribution of EGFR receptor during mitosis generates diverse CNS progenitor cells. Neuron. 2005; 45:873–886. [PubMed: 15797549]
67. Nishiyama A, Watanabe M, Yang Z, et al. Identity, distribution, and development of polydendrocytes: NG2-expressing glial cells. J Neurocytol. 2002; 31:437–455. [PubMed: 14501215]
68. Butt AM, Hamilton N, Hubbard P, et al. Synantocytes: the fifth element. J Anat. 2005; 207:695–706. [PubMed: 16367797]
69. Bergles DE, Roberts JD, Somogyi P, et al. Glutamatergic synapses on oligodendrocyte precursor cells in the hippocampus. Nature. 2000; 405:187–191. [PubMed: 10821275]
70. Ziskin JL, Nishiyama A, Rubio M, et al. Vesicular release of glutamate from unmyelinated axons in white matter. Nat Neurosci. 2007; 10:321–330. [PubMed: 17293857]
71. Ge WP, Zhou W, Luo Q, et al. Dividing glial cells maintain differentiated properties including complex morphology and functional synapses. Proc Natl Acad Sci U S A. 2008
72. Butt AM, Duncan A, Hornby MF, et al. Cells expressing the NG2 antigen contact nodes of Ranvier in adult CNS white matter. Glia. 1999; 26:84–91. [PubMed: 10088675]
73. Butt AM, Kiff J, Hubbard P, et al. Synantocytes: new functions for novel NG2 expressing glia. J Neurocytol. 2002; 31:551–565. [PubMed: 14501223]
74. Kolb B, Morshead C, Gonzalez C, et al. Growth factor-stimulated generation of new cortical tissue and functional recovery after stroke damage to the motor cortex of rats. J Cereb Blood Flow Metab. 2007; 27:983–997. [PubMed: 16985505]
75. Keirstead HS. Stem cells for the treatment of myelin loss. Trends Neurosci. 2005; 28:677–683. [PubMed: 16213602]
76. Pluchino S, Martino G. The therapeutic use of stem cells for myelin repair in autoimmune demyelinating disorders. J Neurol Sci. 2005; 233:117–119. [PubMed: 15896808]
77. Ashton-Chess J, Brouard S, Soulillou JP. Is clinical tolerance realistic in the next decade? Transpl Int. 2006; 19:539–548. [PubMed: 16764632]
78. Barker RA, Widner H. Immune problems in central nervous system cell therapy. NeuroRx. 2004; 1:472–481. [PubMed: 15717048]

79. D'Intino G, Perretta G, Taglioni A, et al. Endogenous stem and precursor cells for demyelinating diseases: an alternative for transplantation? Neurol Res. 2006; 28:513–517. [PubMed: 16808881]

80. Nait-Oumesmar B, Picard-Riera N, Kerninon C, et al. Activation of the subventricular zone in multiple sclerosis: evidence for early glial progenitors. Proc Natl Acad Sci U S A. 2007; 104:4694–4699. [PubMed: 17360586]

81. Blakemore WF, Franklin RJ. Transplantation options for therapeutic central nervous system remyelination. Cell Transplant. 2000; 9:289–294. [PubMed: 10811401]

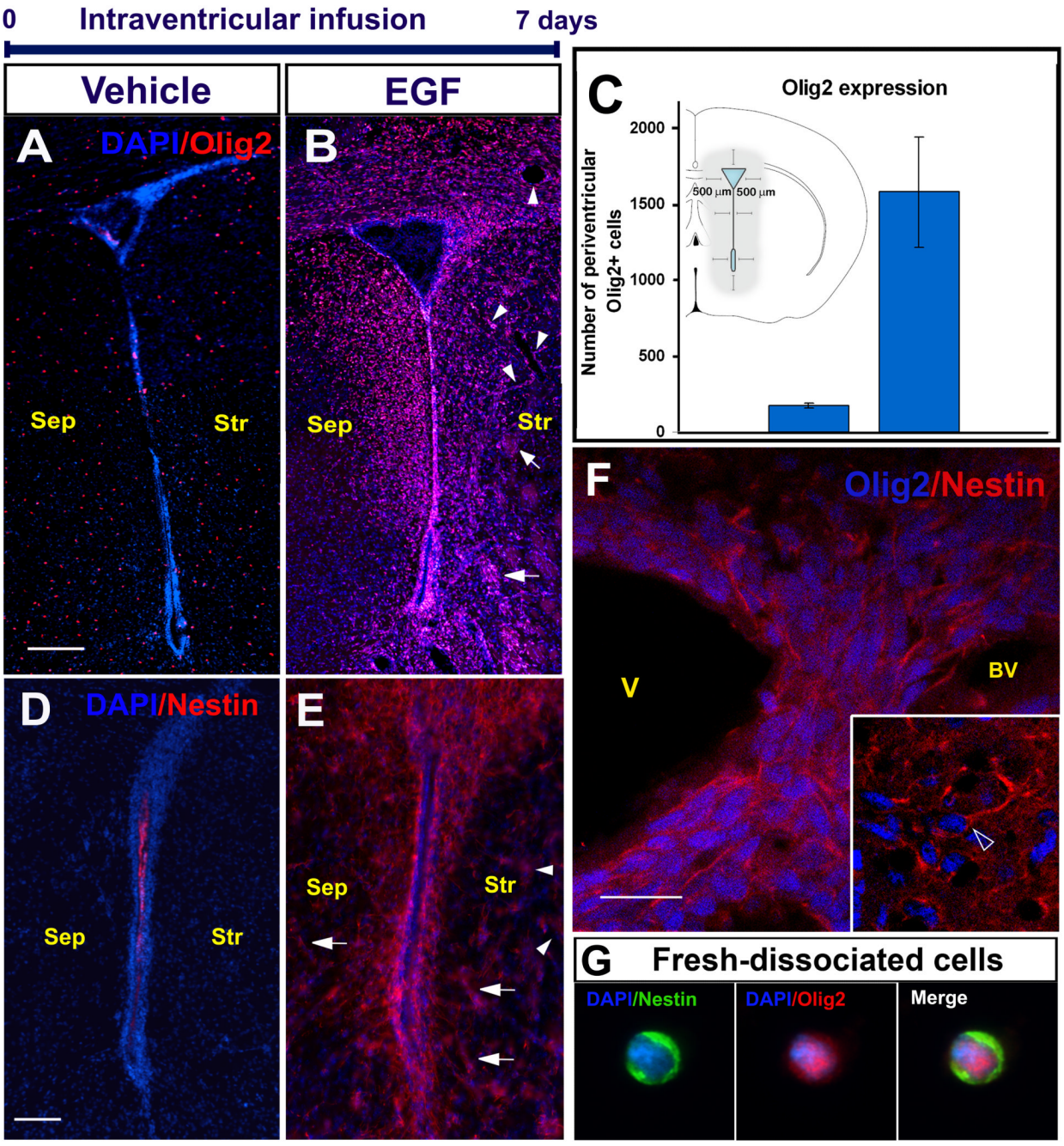

Figure 1.

EGF effects after a 7-day intraventricular infusion. Olig2 periventricular expression in the vehicle (A) and (B) EGF group. Olig2+ cells are aligned along blood vessels (BV; arrow heads) and myelin tracts of the striatum (Str; arrows). C: EGF increases 9.6-fold the Olig2+ expression (Student's "t" test; $P < 0.05$). The inserted drawing depicts the area used for quantifications. Nestin periventricular expression in (D) vehicle- and (E) EGF- infused animals. Nestin expression was also found along blood vessels (arrow heads), and myelin tracts (arrows). F: Olig2/nestin co-expression in the periventricular region (main square). Inset: Olig2+ cell showing a nestin+ leading process (open arrow head). G: Periventricular

cell freshly dissociated and immunostained. Sep: Septum; V: Ventricle. Scale bar in A, B, D, E = 200 μm; F and inset = 20 μm.

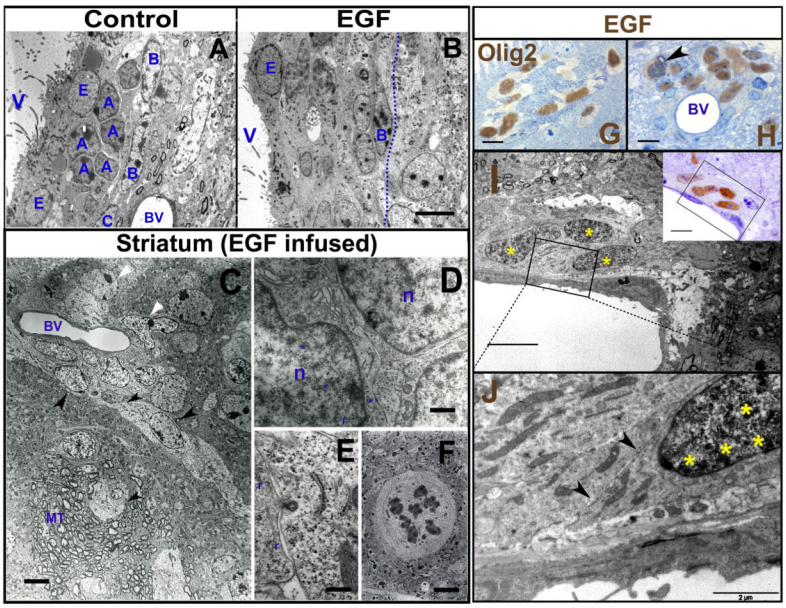

Figure 2. Ultrastructural characterization of EIPs

No type-A and type-C cells are found in the EGF-infused group (**B**) as compared to the control group (**A**). **C:** Parenchymal astrocytes (white arrow heads) and EIPs (black arrow heads). EIPs infiltrate myelin tracts (MT) and blood vessels (BV). These cells have abundant ribosomes (*r*) (**F**), desmosome-like contacts (blue asterisks), endocytic vesicles (**F**) and mitoses (**G**). **G - H:** Olig2 pre-embedding ICC; DAB brown precipitates show the Olig2 expression. **I - J:** DAB precipitates detected by EM (yellow asterisks). The EM section was obtained from the semi-thin section shown in the inset. V: Ventricle; n: Nucleus. Scale bars: A, B, G - I and inset = 10 μm; C = 5 μm; D = 0.5 μm; E - F = 1 μm; J = 2 μm.

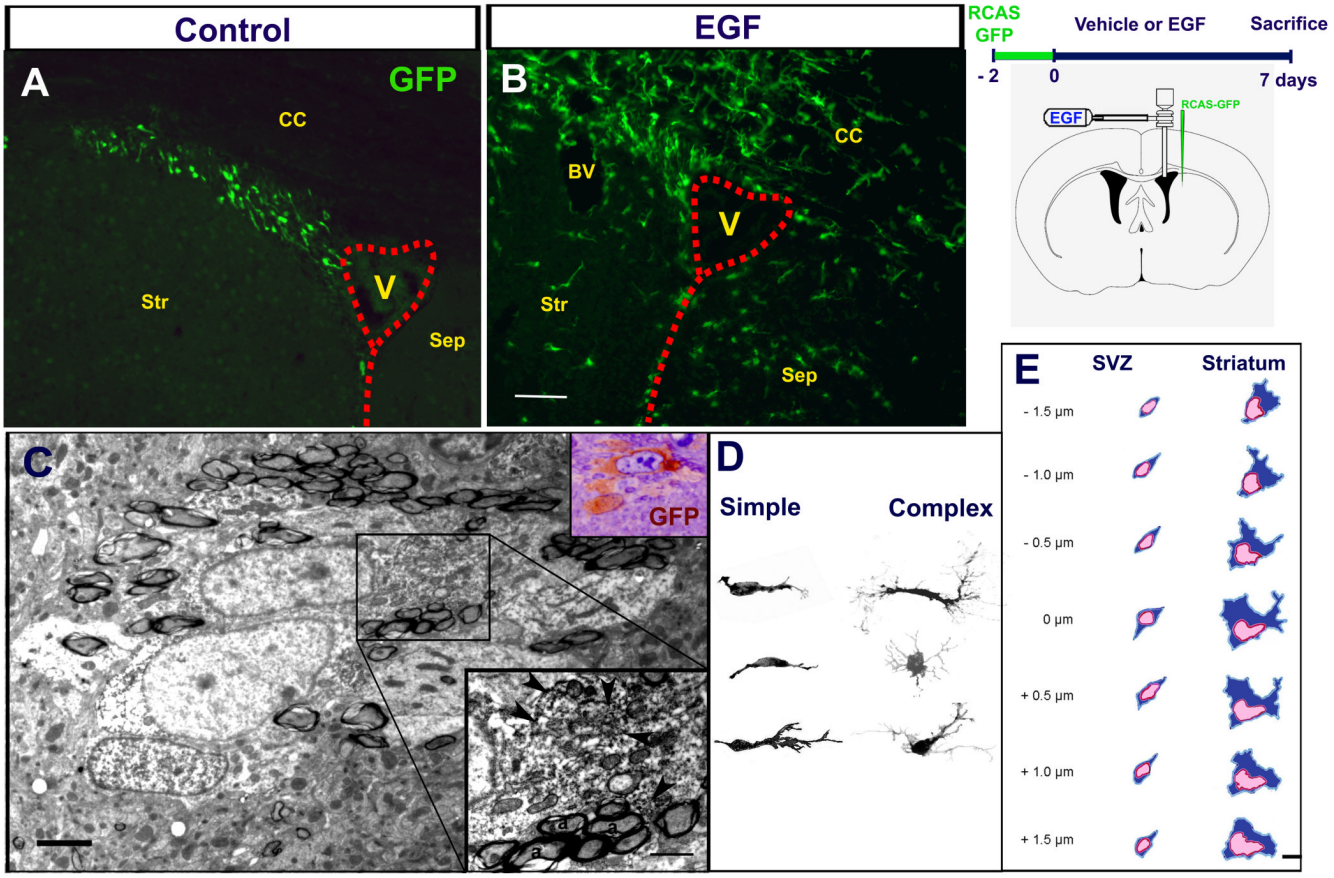

Figure 3. SVZ astrocytic stem cells give rise to EIPs

GFP-expressing cells after vehicle (**A**) and EGF (**B**) infusions. A number of GFP+ cells derived from the SVZ astrocytes were observed around the lateral ventricle (V) and infiltrated the brain parenchyma of EGF-infused animals. **C.** Axonal tracts showing two GFP-labeled cells analyzed by EM. Upper inset shows the semi-thin section from where the ultrathin section was obtained. Lower inset: Higher magnification of the area indicated in C; arrowheads indicate DAB precipitates. **D:** Z-stack reconstructions of GFP+ cells. **E:** Schematic 3-D reconstructions by EM. The numbers at the left indicate the distance between each section. Time line and mouse brain schematic drawing that shows the cannula's spatial position and the injection site to label SVZ astrocytes CC: Corpus callosum; Str: Striatum; Sep: Septum; BV: Blood vessel. Scale bar in B = 100 µm; C = 2.5 µm, inset = 1 µm; E = 5 µm.

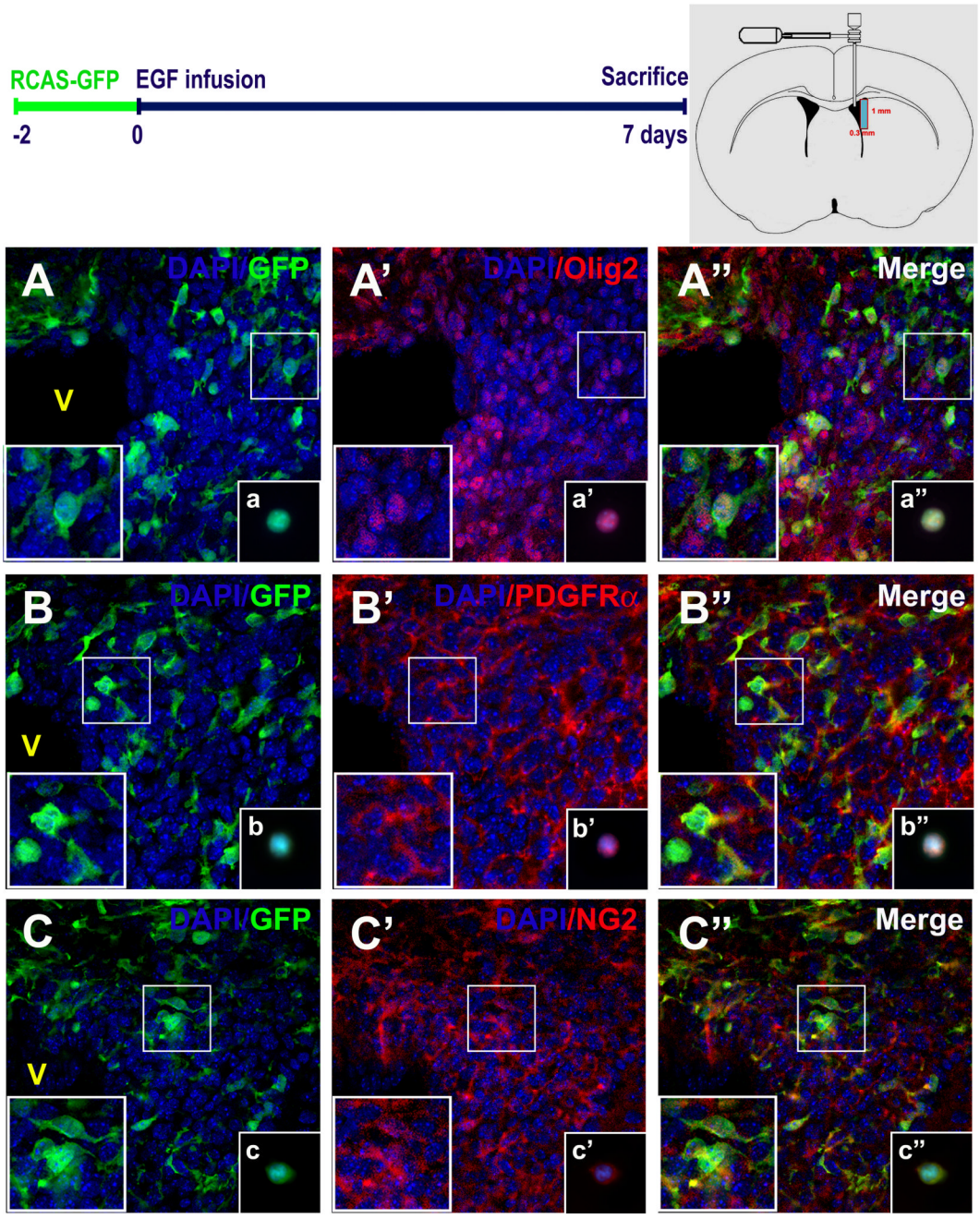

Figure 4. EIPs express markers related to oligodendrocyte lineage

Brain sections were co-stained with anti-GFP and anti-Olig2 (**A - A"**), anti-PDGRFα (**B - B"**), and anti- NG2 (**C - C"**) antibodies. High magnification cell details are shown at bottom left square. Independent experiments and immunolabelings were performed on freshly-dissociated cells (insets: **a-a", b-b", c-c"**). Schematic brain drawing depicts the dissected area (1mm × 0.3 mm) where fresh-dissociated cells were obtained. Nuclear staining was performed with DAPI (blue). V: Ventricle. Scale bars = 20 μm.

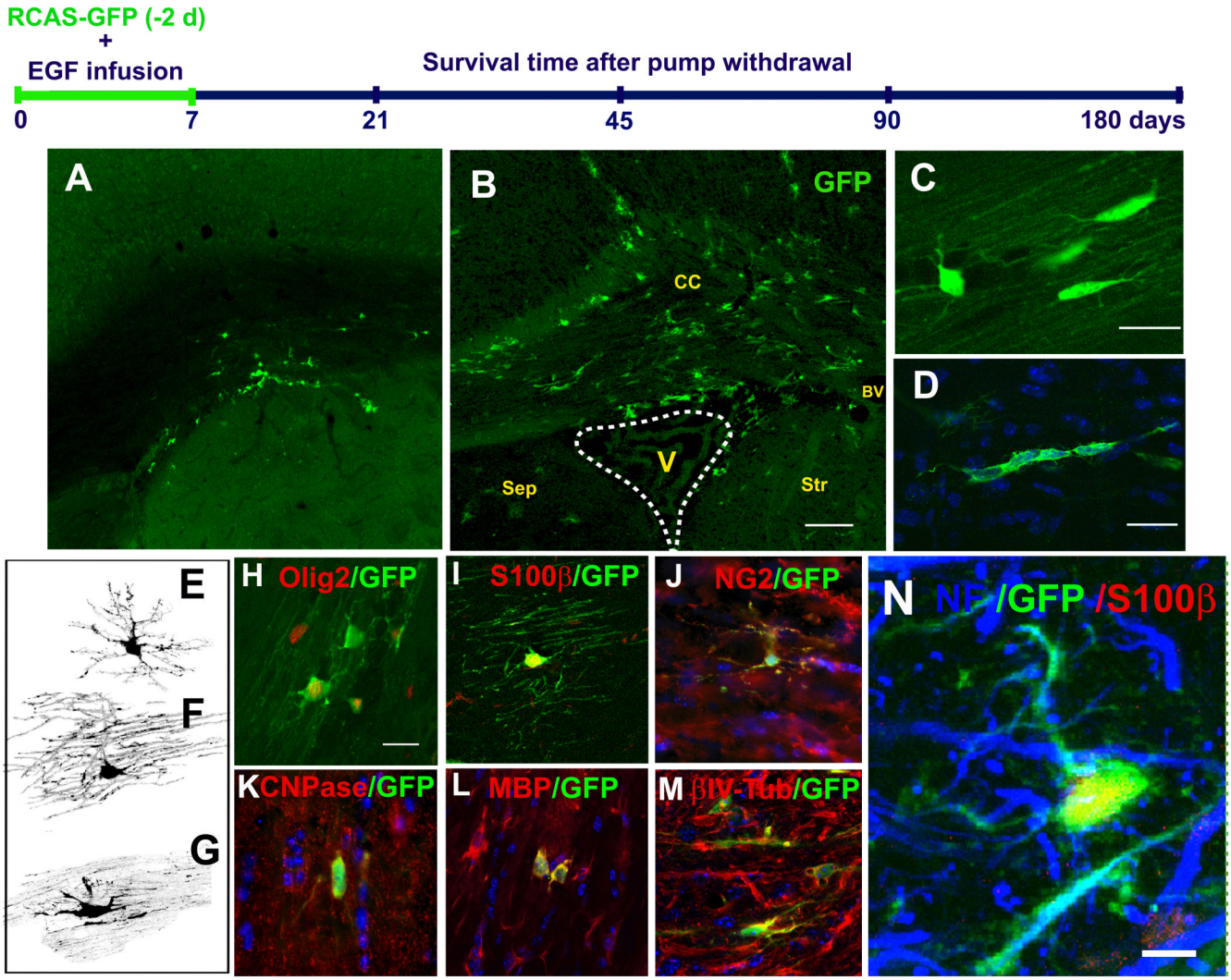

Figure 5. EIPs derived from SVZ astrocytes give rise to oligodendrocytes

Schematic timeline shows the experimental design. GFP+ cells found in the brain parenchyma, 21 days after infusion of vehicle (**A**) or EGF (**B**). In the corpus callosum (CC) many cells had characteristic of pre-myelinating and myelinating oligodendrocytes (**C**) that frequently formed cellular "cords" (**D**). Similar findings were observed in all regions at every time point. **E - G:** Confocal Z-stack 3D reconstructions of the GFP+ cells found in the corpus callosum. **H - N**: Markers expressed by RCAS-GFP-labeled cells found in the corpus callosum. These cells have a close relationship with neurofilaments (NF) (**N**). Sep: Septum, Str: Striatum, BV: Blood vessel. V: Ventricle. Scale bar in A-B = 100 μm; B, C, G - K = 20 μm; N = 5 μm.

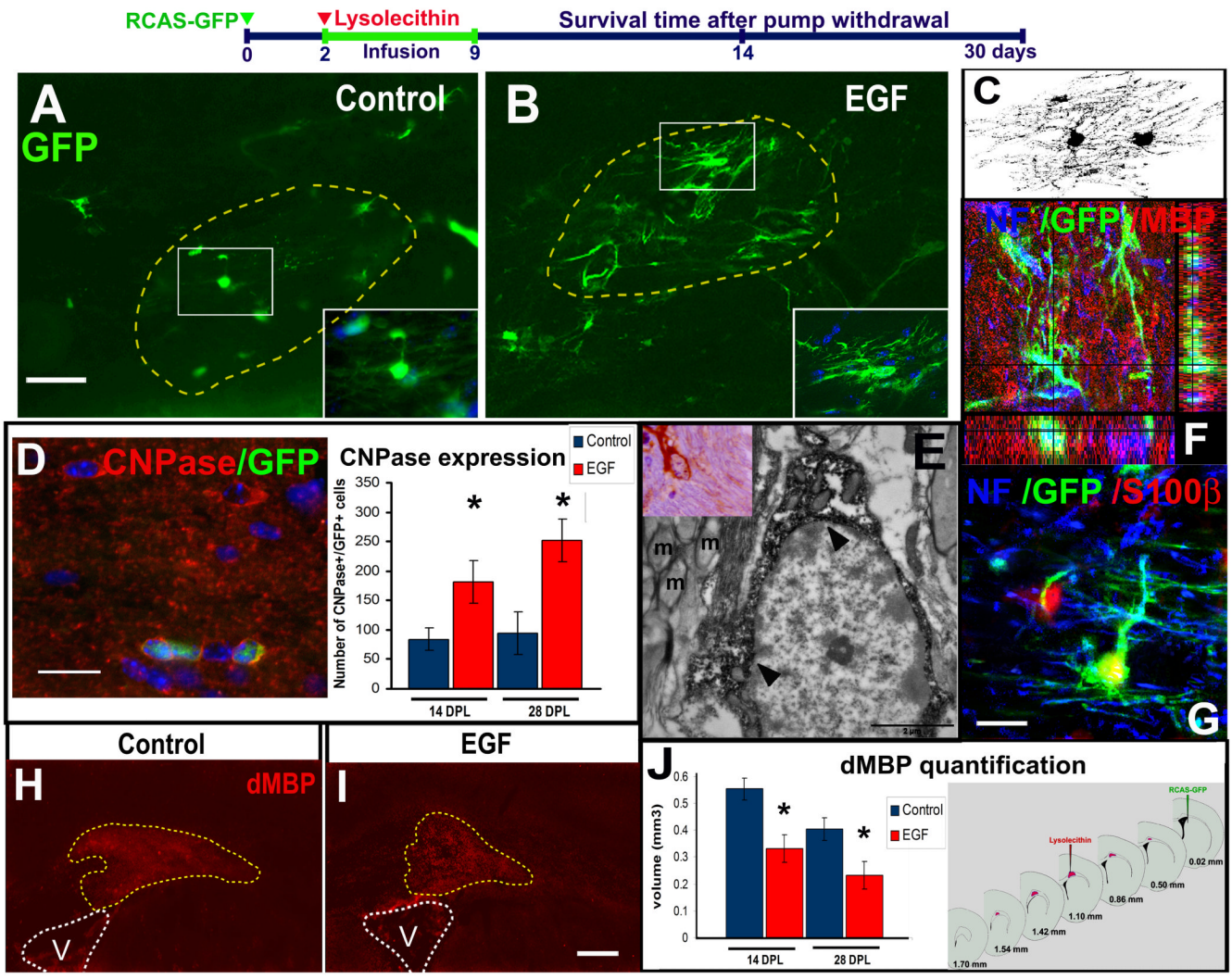

Figure 6. EIPs derived from SVZ B cells promote remyelination

Schematic timeline shows the experimental design. GFP+ oligodendrocytes found in the demyelinated area (dotted line) of the EGF group (**B**) and the control-group (**A**) 14 days post-lysolecithin injection (DPL). C: Confocal Z-stack reconstruction of two cells found in the demyelinated area of an EGF-infused animal. GFP+ cells expressed CNPase (**D**), MBP (**F**) or S100β (**G**). Ultrastructure of GFP+ cells suggests they correspond to oligodendrocytes (**E**). The number of CNPase+GFP+ cells in the EGF-infused animals was higher than the control-vehicle group at 14 and 28 DPL (**D**) ($P < 0.05$; Student "*t*" test). dMBP expression at 14 DPL in a control- (**H**) and EGF- (**I**) infused animal. Volume of dMBP+ lesion was reduced by the effect of EGF infusion (**J**). NF: Neurofilaments; V: Ventricle; m: myelinated axon. Bars A - B = 50 μm; D = 20 μm; E - F = 10 μm; G-H = 200 μm.

Table 1

Expression of oligodendrocyte lineage markers in the corpus callosum after epidural growth factor removal[a]

Days after pump withdrawal	Septum				Striatum				Cortex			
	CNPase	Olig2	NG2	S100β	CNPase	Olig2	NG2	S100β	CNPase	Olig2	NG2	S100β
21 days (n = 4 per group)												
Control	0	6 ± 2	5 ± 5	0	0.3 ± 0.5	2 ± 2	6 ± 3	1 ± 1	1 ± 2	6 ± 3	5 ± 1	5 ± 3
EGF	14 ± 4[b]	13 ± 3[b]	15 ± 2[b]	21 ± 5[b]	4 ± 2[b]	20 ± 6[b]	20 ± 6[b]	41 ± 4[b]	3 ± 1	48 ± 5[b]	18 ± 2[b]	60 ± 8[b]
45 days (n = 4 per group)												
Control	0	1 ± 1	2 ± 2	0	0	1 ± 2	2 ± 4	1 ± 1	0	2 ± 1	2 ± 2	3 ± 2
EGF	9 ± 2[b]	37 ± 4[b]	20 ± 8[b]	25 ± 7[b]	9 ± 1[b]	24 ± 6[b]	18 ± 6[b]	39 ± 15[b]	7 ± 3[b]	71 ± 5[b]	14 ± 4[b]	71 ± 6[b]
90 days (n = 3 per group)												
Control	0.3 ± 0.6	1 ± 15	1 ± 1	0	0	1 ± 2	2 ± 1	0.3 ± 0.5	1 ± 1	1 ± 2	1 ± 1	2 ± 1
EGF	4 ± 2[b]	42 ± 4[b]	27 ± 8[b]	38 ± 8[b]	9 ± 2[b]	38 ± 6[b]	25 ± 5[b]	46 ± 12[b]	13 ± 3[b]	72 ± 18[b]	19 ± 4[b]	76 ± 27[b]
180 days (n = 3 per group)												
Control	0	0	1 ± 1	0	0	1 ± 2	1 ± 1	0	0	1 ± 1	1 ± 1	2 ± 1
EGF	6 ± 3[b]	48 ± 7[b]	32 ± 5[b]	41 ± 9[b]	7 ± 2[b]	44 ± 7[b]	28 ± 8[b]	52 ± 7[b]	10 ± 1[b]	89 ± 7[b]	21 ± 7[b]	100 ± 22[b]

Abbreviations: EGF, epidermal growth factor.

[a]The values of each marker correspond to the total number of cells quantified in ten 30-lm consecutive sections, each spaced 180 lm apart.

[b]Statistical difference between the EGF groups vs. controls ($p < 0.05$; Student's t test).

Stem Cells. Author manuscript; available in PMC 2012 May 07.